

Gauge-invariant two- and three- density correlators*

C. Alexandrou^a, Ph. de Forcrand^b and A. Tsapalis^c

^aDepartment of Physics, University of Cyprus, CY-1678 Nicosia, Cyprus

^bETH-Zürich, CH-8093 Zürich and CERN Theory Division, CH-1211 Geneva 23, Switzerland

^cDepartment of Physics, University of Wuppertal, Wuppertal, Germany

Gauge-invariant spatial correlations between two and three quarks inside a hadron are measured within quenched and unquenched QCD. These correlators provide information on the shape and multipole moments of the pion, the rho, the nucleon and the Δ .

1. Introduction

Gauge-invariant two- and three-density correlators inside a hadron reduce to the square of the wave function in the non-relativistic limit, yielding detailed information on hadron structure. Quark spatial distributions, hadronic shapes, charge radii, etc., can be extracted. An interesting question is whether the nucleon is deformed. Strong evidence for deformation in the nucleon and/or Δ is provided by recent accurate measurements [1] in photoproduction experiments on the nucleon. One can compare with the experimental results by calculating the N to Δ^+ transition form factors [2]. Moreover, the Δ^+ deformation can be directly obtained from the wave function. The nucleon, however, has zero spectroscopic quadrupole moment, since it is a spin 1/2 particle. This implies that any deformation that intrinsically may be present for a given background gauge field will average out to zero in the gauge configuration ensemble.

2. Observables

In this work we consider equal-time correlators. For a meson we calculate the matrix element

$$C_\Gamma(\mathbf{r}, t) = \int d^3r' \langle M | \rho^u(\mathbf{r}', t) \rho^d(\mathbf{r}' + \mathbf{r}, t) | M \rangle \quad (1)$$

with $\rho_\Gamma^u(\mathbf{r}, t) =: \bar{u}(\mathbf{r}, t) \Gamma u(\mathbf{r}, t) :.$ We take $\Gamma = \gamma_0$ for the normal ordered charge density operator, and $\mathbf{1}$ for the matter density. In the non-relativistic limit this allows to extract respectively

the charge and matter density distributions. Unlike Bethe-Salpeter amplitudes, these correlators are gauge-invariant. Here we take the u - and d -quarks to be degenerate in mass.

The form factors $F(\mathbf{q}^2)$ at low momenta can be extracted from the Fourier transform of the charge density-density correlator [3]

$$\begin{aligned} Q(\mathbf{q}^2) &= \int_0^\infty d^3r \exp(i\mathbf{q}\cdot\mathbf{r}) C_{\gamma_0}(\mathbf{r}, t) / 2m_\pi \\ &\rightarrow \frac{(E + m_\pi)^2}{4Em_\pi} F(\mathbf{q}^2)^2 \quad . \end{aligned} \quad (2)$$

For baryons the charge distribution is obtained by using three density insertions. This involves two relative distances and it is computed efficiently by using FFT. The diagrams involved are shown in Fig. 2. The top right diagram requires the all-to-all propagator [4] and will not be considered here. We check that the contribution of this diagram is small by comparing the integrated one-particle density $\int d^3r_2 C(\mathbf{r}_1, \mathbf{r}_2, t)$ with the two-density correlator, $\int d^3r' \langle h | \rho^d(\mathbf{r}', t) \rho^u(\mathbf{r}' + \mathbf{r}_1, t) | h \rangle$, shown by the lower diagram of Fig. 2.

3. Results

We first discuss the results obtained in the quenched approximation at $\beta = 6.0$ for a lattice of size $16^3 \times 32$. The parameters of the simulation for both quenched and unquenched calculations are summarized in the following Table.

The charge and matter density distributions for the pion and the rho mesons are shown in Fig. 2 at

*Talk presented by C. Alexandrou.

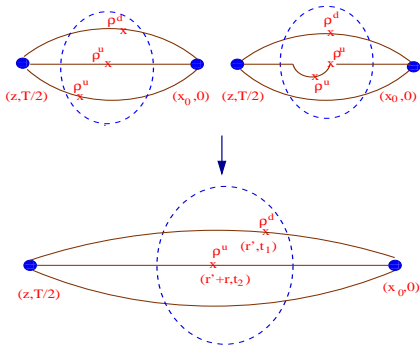


Figure 1. Three-density correlator for a baryon where all the insertions are taken at equal times t . t and $T/2 - t$ are taken large enough to filter out the excited baryonic states.

Quenched			Unquenched(from [5])		
κ	m_π/m_ρ	#confs.	κ_{sea}	m_π/m_ρ	#confs.
0.153	0.81	220	0.156	0.83	150
0.154	0.78	220	0.157	0.76	200

$\kappa = 0.154$. We find that the charge distribution is broader than the matter distribution, in agreement with Ref. [6]. The matter distributions for the pion and the rho are almost identical, but the density distribution is considerably broader for the rho. As seen in Fig. 3, the nucleon and the Δ^+ have very similar matter distributions to the rho meson, whereas larger variations are visible in the charge density distributions.

In Fig. 4 we show the pion form factor which, being the simplest, can be reliably extracted from our set of data. Its low momentum behaviour is well described by the vector dominance result $F(\mathbf{q}^2) \sim 1/(1 + \mathbf{q}^2/m^2)$. We observe a weak dependence on κ obtaining 0.57, 0.59 and 0.61 GeV at $\kappa = 0.153, 0.1554$ and 0.155 respectively. Extrapolating linearly in m_π^2 we obtain $m \sim 0.65$ GeV within 15% of the rho meson mass.

Hadron deformation can be investigated by evaluating the root mean squared (rms) radius along the spin axis and perpendicular to it. We show the charge rms radii in Fig. 5 as a function of the quark mass. The pion, having equal rms radii, is spherical whereas for the rho the asymmetry between the longitudinal and transverse radii increases as we approach the chiral limit. A reliable extrapolation to the chiral limit needs lighter quarks and a larger lattice to contain the rho. A similar analysis for the nucleon shows that it is

spherical as expected, whereas the Δ^+ shows no statistically significant deformation [4]. The rms radii computed from the matter distribution show no such deformation also in the case of the rho.

We now compare our quenched results for the charge correlator with those obtained using two degenerate flavors of Wilson fermions, with similar lattice spacing and m_π/m_ρ values. Fig. 6 shows that unquenching leaves the pion unchanged, whereas the rho, the nucleon and the Δ^+ become broader. The asymmetry in the rho increases as seen by comparing the longitudinal and transverse radii in Fig. 5. The Δ^+ shows a small asymmetry which points to pion cloud contributions to the deformation.

The three-density charge correlator was computed in the quenched approximation using 30 configurations at $\kappa = 0.15$ and 0.154. More detailed information on hadron structure can be extracted from this correlator. As an example we show in Fig. 7 the u - and d - quark spatial distributions. The systematically broader d -quark distribution gives rise to a negative neutron rms charge radius.

4. Conclusions

We have presented a gauge-invariant determination of hadron charge and matter density distributions. The main conclusions from this study are the following: 1) The matter density distribution is very similar for the π, ρ , nucleon and Δ^+ , unlike the charge density which is narrower for the pion than for the rest. In all cases the charge density distribution is broader than the matter density distribution. 2) Vector dominance provides a good description of the pion form factor at low momenta. 3) Unquenching leaves the pion size unchanged but the rho, the nucleon and Δ^+ become broader. 4) In the quenched approximation the rho in the 0-spin projection is prolate whereas the Δ^+ has no statistically significant deformation. 5) Unquenching increases the rho deformation and produces a small deformation for the Δ^+ with the $+3/2$ spin state being slightly oblate. 6) The d -quark spatial distribution in the neutron extracted from the three density correlator is broader than that of the u -quark, thus accounting for the negative rms charge radius of

the neutron.

REFERENCES

- [1] C. Mertz *et al.*, Phys. Rev. Lett. **86** (2001) 2963; K. Joo *et al.*, Phys. Rev. Lett. **88** (2002) 122001.
- [2] See talk by A. Tsapalis, C. Alexandrou *et al.*, these proceedings.
- [3] W. Wilcox, Phys. Rev. D **43**, 2443 (1991).
- [4] C. Alexandrou, Ph. de Forcrand and A. Tsapalis, hep-lat/0206026.
- [5] N. Eicker *et al.*, Phys. Rev. D **59** (1999) 014509.
- [6] A. Green, J. Koponen, P. Pennanen, C. Michael, hep-lat/0206015.

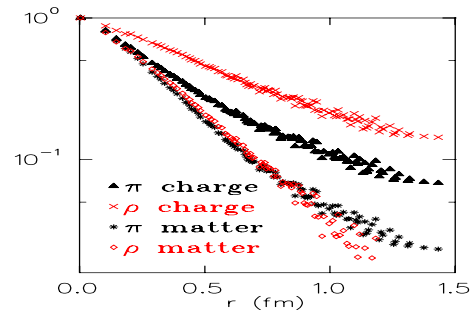


Figure 2. Charge and matter density distributions at $\kappa = 0.154$ for the pion and the rho.

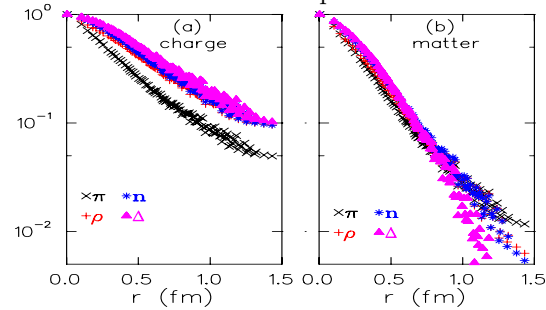


Figure 3. Charge and matter density distributions at $\kappa = 0.153$.

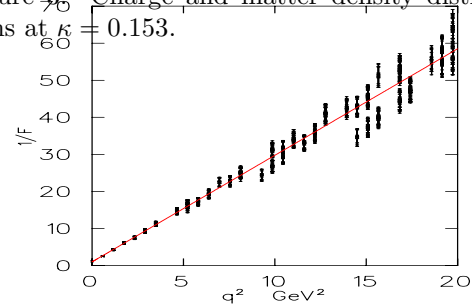


Figure 4. $1/F(\mathbf{q}^2)$ versus \mathbf{q}^2 at $\kappa = 0.154$. The solid line is a fit to the form $(1 + \mathbf{q}^2/m^2)$.

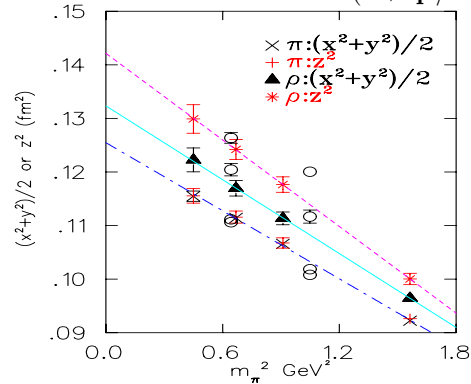


Figure 5. $\langle z^2 \rangle$ and $\langle (x^2 + y^2) / 2 \rangle$ vs the pion mass squared. The lines are linear fits to the quenched data. The empty circles show full QCD results.

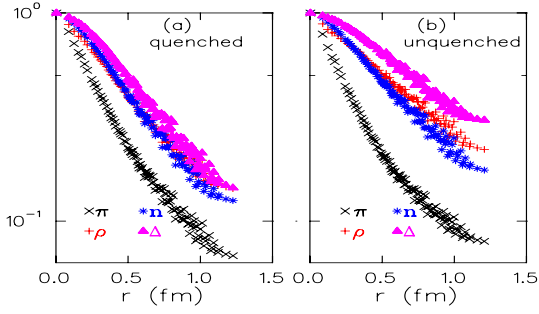


Figure 6. (a) Density-density correlators, $C_{\gamma_0}(\mathbf{r})$, for the pion, the rho, the nucleon and the Δ^+ at $\kappa = 0.154$ vs $|\mathbf{r}|$. (b) Same as (a) but with two dynamical quark flavors at $\kappa = 0.157$. Errors bars are omitted for clarity.

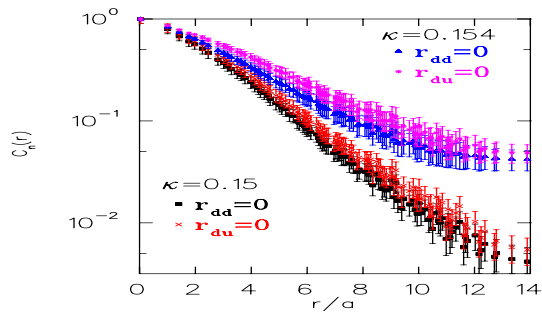


Figure 7. The u - and d - distributions inside the neutron for $\kappa = 0.15$ and 0.154 .